*Regular Paper*

**Title:**

# Searching for Acrolein-Scavenging Compounds in Plants: Isoalliin from Onion as an Excellent Scavenger

**Running head:**

Acrolein scavenging compounds in plants

**Authors:**

Ayako Hada [a], Chihiro Nozaki [b], Natsumi Tamura [b], Kenji Matsui [a], Yasumasa Matsuoka [c], Daisuke Shibata [d#], Jun'ichi Mano [a,e,f*†]

**Affiliations:**

[a] Graduate School of Sciences and Technology for Innovation, Yamaguchi University, Yoshida 1677-1, Yamaguchi 753-8515, Japan

[b] Faculty of Agriculture, Yamaguchi University, Yoshida 1677-1, Yamaguchi 753-8515, Japan

[c] Advanced Technology Institute, Yamaguchi University, Yoshida 1677-1, Yamaguchi 753-8515, Japan

[d] Kazusa DNA Research Institute, 2-6-7 Kazusa-kamatari, Kisarazu Chiba, 292-0818 Japan

[e] Science Research Center, Organization for Research Initiatives, Yamaguchi University, Yoshida 1677-1, Yamaguchi 753-8515, Japan

[f] The United Graduate School of Agricultural Science, Tottori University, Tottori 680-8553 Japan

***Corresponding author:** Jun'ichi Mano

E-mail: mano@yamaguchi-u.ac.jp

# **Present address:** The Institute of Advanced Energy, Kyoto University, Gokasho, Uji, 611-0011 Japan

†**Present address:** Graduate School of Agriculture, Kobe University, Rokkodai-cho 1-1, Kobe, 657-8501 Japan

**ABSTRACT**

Reactive carbonyl species (RCS), such as acrolein (Acr), are generated via the degradation of lipid peroxides and function both as signaling molecules and as cytotoxins downstream of reactive oxygen species (ROS). The aim of this study was to identify RCS-scavenging compounds, acting as secondary antioxidants, in plants. We established an HPLC-based method to sensitively evaluate the RCS-scavenging ability of compounds, using Acr as a representative RCS. Among 80% ethanol extracts of 46 angiosperm species, the highest scavenging activities were observed in garlic, spinach, avocado, broccoli, and lotus, representing a diverse range of plant families. The active ingredient from garlic cloves was identified as *S*-allyl cysteine sulfoxide (alliin), an amino acid typical of *Allium* species, which trapped up to two Acr molecules at its amino group. Notably, *S*-(1*E*)-propenyl cysteine sulfoxide (isoalliin), a structural analog of alliin and a major constituent of onion, showed even stronger Acr-scavenging activity. Isoalliin outperformed known Acr scavengers such as carnosine, epigallocatechin gallate, resveratrol, and hesperetin. These findings highlight isoalliin as a representative plant-derived RCS scavenger and emphasize the importance of *S*-alk(en)yl cysteine sulfoxides as potent Acr-scavenging compounds in plants. This study further suggests that structurally diverse RCS scavengers remain to be discovered among specialized metabolites in the plant kingdom.

**KEYWORDS:** *acrolein*, *alliin*, *isoalliin*, *methiin*, *reactive carbonyl species*

54 Plant life is exposed to potential threats from reactive oxygen species (ROS). During
55 photosynthesis in plants, singlet oxygen ($^1O_2$) and superoxide radical ($O_2^-$) are constantly
56 produced in chloroplasts (Asada 2006). Furthermore, the $H_2O_2$ generation flux in
57 peroxisomes in illuminated leaves of C3 plants reaches 25% of the flux of $CO_2$ fixation on
58 electron base. This is approximately 50 times greater than the ROS generation flux associated
59 with mitochondrial respiration (Foyer and Noctor, 2003). When plants suffer environmental
60 stress, i.e. any changes in the surrounding environmental conditions that are not favorable for
61 a plant, ROS production in the cells are increased due to the disturbance of metabolism (for
62 example, the rate of $CO_2$ fixation in leaves decreases at low temperatures or under drought).
63 ROS oxidize biomolecules such as proteins, nucleic acids and lipids, thereby impairing their
64 functions and damaging cells. As a defense system against ROS, plant cells are richly
65 equipped with multiple types of ROS-scavenging enzymes and antioxidants, thereby keeping
66 ROS concentrations low enough.
67 ROS exert their biological functions also via the secondary products 'reactive carbonyl
68 species (RCS)'. RCS is a collective name of the $\alpha,\beta$-unsaturated aldehydes and ketones such
69 as acrolein (Acr) and 4-hydroxy-(*E*)-2-nonenal (HNE) that are formed via the degradation of
70 lipid peroxides (Esterbauer et al. 1991, Aldini et al. 2005, Mano 2012). An RCS molecule
71 readily forms an adduct with a protein at the thiol-, amino-, or imidazole group via Michael
72 addition of its $\beta$-carbon (Esterbauer et al. 1991), and cause alterations of the protein function

73 (Wible and Sutter 2017). In plants, more than a dozen types of RCS occur (Schauenstein et
74 al. 1977, Mano 2012) and their levels are increased under oxidative stress conditions (Yin et
75 al. 2010, Yamauchi et al. 2012, Biswas and Mano 2015, Roach et al. 2018, Sultana et al.
76 2022, 2024). Rises of RCS levels have significant physiological impacts. For example, the
77 genetic enhancement of the RCS-scavenging enzyme 2-alkenal reductase (AER) (Mano et al.
78 2002, 2005) in transgenic plants suppressed the increases in RCS levels due to salt stress
79 (Sultana et al. 2024), aluminium stress (Yin et al. 2010) and light stress (Mano et al. 2010)
80 and thereby conferred stress tolerance. Vice versa, the genetic deficiency of aldehyde
81 alkenal/one reductase (Yamauchi et al. 2012) and aldehyde oxidase (Srivastava et al. 2017,
82 Nurbekova et al. 2021) made the plants more susceptible to oxidative stress or senescence.
83 The plant defense system against RCS toxicity consists of several types of enzymes and small
84 molecules, as the system against ROS. As for enzymatic defense, several classes of enzymes
85 with distinct RCS-detoxifying reactions have been characterized such as AER (Mano et al.
86 2002, 2005), glutathione transferase tau isozymes (Mano et al. 2017, 2019a,b) and aldehyde-
87 scavenging enzymes such as aldo-keto reductase (Yamauchi et al. 2011), aldehyde
88 dehydrogenase (Sunker et al. 2003) and aldehyde oxidase (Srivastava et al. 2017, Nurbekova
89 et al. 2021).
90 RCS-scavenging small molecules also occur in plants. Thiol compounds such as cysteine
91 (Cys) and the reduced form of glutathione are excellent RCS scavengers (Esterbauer et al.

92 1975). Various polyphenols also have the RCS scavenging ability. Zhu et al. (2009)
93 compared the RCS scavenging ability of a dozen tea polyphenols *in vitro* and found that nine
94 of them, including epigallocatechin gallate (EGCG), showed a high Acr-scavenging activity.
95 The reaction of EGCG and Acr starts with a nucleophilic attack of the carbon at position 8 on
96 the EGCG A-ring on the *β*-carbon of Acr, thus forming a Michael adduct. Subsequent aldol
97 condensation produces a ring structure (Huang, et al., 2020). One EGCG molecule can bind
98 up to three Acr molecules (Sugimoto, et al., 2021). Acr-scavenging reactions have been also
99 characterized for other polyphenols and their glycosides such as resveratrol, hesperetin
100 (Wang, et al., 2015), ferulic acid (Tao, et al., 2019), pelargonidin (Colzani, et al., 2018),
101 myricetin (Zhang, et al., 2020) and cyanidin-3-*O*-glucoside (Song, et al., 2021).
102 Amino compounds also have RCS-scavenging potential. The primary amino group in γ-
103 aminobutyric acid (GABA), L-Ala and L-Ser serves as a Michael acceptor to bind up to two
104 molecules of Acr (Jiang et al. 2020a, Zou et al. 2021). Recently it was reported that *S*-allyl
105 cysteine sulfoxide (alliin), an amino acid typical of *Allium* species, can scavenge Acr at a
106 high speed although the reaction mechanism has yet to be clarified (Uemura et al. 2023).
107 Theophylline, a purine derivative found in tea, forms a Michael adduct between its secondary
108 amine and the *β*-carbon of Acr at a high rate (Jiang, et al., 2020b). Interestingly, animals
109 contain RCS-scavenging dipeptides carnosine, homocarnosine, and anserine (Aldini et al.
110 2002) in brain and muscle. The amino and imidazole groups of these histidine-containing

111 dipeptides react as Michael acceptors (Aldini et al., 2005), allowing them to be excellent RCS
112 scavengers (Aldini et al., 2002; Liu et al., 2003; Carini et al., 2003). Exogenous application
113 of these dipeptides to plant cells or seedlings suppressed the RCS levels and mitigated
114 oxidative injury, without affecting ROS levels (Biswas and Mano, 2015; Sultana et al., 2022),
115 showing that RCS-scavenging compounds can protect plants as the "secondary antioxidants".
116 In this study, we aimed at discovering RCS-scavenging compounds in plants. Employing Acr
117 as a representative RCS, we evaluated RCS-scavenging ability of dozens of angiosperms.
118 Garlic cloves showed the highest content of Acr-scavenging ability, which was attributed to
119 alliin, a garlic-typical amino acid. We found that isoalliin and methiin, the cysteine
120 derivatives relative to alliin, also showed excellent Acr-scavenging ability and revealed the
121 reaction mechanism. Potential of plant specialized compounds as the secondary antioxidants
122 is discussed.
123

124 **Materials and Methods**

125 ***Chemicals*** Alliin and methiin were purchased from LKT Laboratories (Saint Paul, MN).
126 Carnosine, fluorescein, and HNE dimethyl acetal (HNE-DMA) were purchased from Sigma-
127 Aldrich Japan (Tokyo), and isoalliin from Nagara Science Co. (Gifu, Japan). Anserine nitrate
128 was purchased from Fujifilm Wako Pure Chemical (Osaka, Japan). 2,4-
129 Dinitrophenylhydrazine (DNPH), purchased from Fujifilm Wako, was purified by

130 recrystallization in acetonitrile and kept in acetonitrile until use (Mano et al. 2022). All other
131 chemicals were of analytical grade. Acr was prepared on the day of use by hydrolysis of the
132 acetal, as follows. Acrolein dimethyl acetal (Tokyo Chemical Industry, Tokyo, Japan) was
133 dissolved in 100 mM HCl aqueous solution at 40˚C for 40 min. The solution was then
134 neutralized with $NaHCO_3$ and further incubated at 25˚C for 2 h. The concentration of Acr was
135 determined from the absorbance at 215 nm with an extinction coefficient of 15.0 $mM^{-1}$ $cm^{-1}$
136 (in water).

137 ***Plant Materials*** Bamboo (*Phyllostachys heterocycla*) shoots and yuzu (*Citrus junos*) fruits
138 were harvested from Yamaguchi University's experimental field. Following materials of fresh
139 plants were purchased from grocery stores in Yamaguchi (Japan) between April and December
140 2018: Apple (*Malus domestica*) fruits, asparagus (*Asparagus officinalis*) shoots, avocado
141 (*Persea americana*) fruits, bell pepper (*Capsicum annuum* 'Grossum') fruits, bitter melon
142 (*Momordica charantia* var. *pavel*) fruits, broccoli (*Brassica oleracea* var. italica) buds, carrot
143 (*Daucus carota* subsp. *sativus*) roots, cherry (*Cerasus avium*) fruits, chestnuts (*Castanea*
144 *crenata*), Chinese yam (*Dioscorea polystachya*) roots, common ginger (*Zingiber officinale*)
145 rhizomes, edible burdock (*Arctium lappa*) roots, eggplant (*Solanum melongena*) fruits, fig
146 (*Ficus carica*) fruits, garlic (*Allium sativum*) cloves, grape (*Vitis labruscana* 'Pione') fruits,
147 green onion (*Allium fistulosum*) leaves, guava (*Psidium guajava*) fruits, Haskap berry
148 (*Lonicera caerulea* var. *emphyllocalyx*) fruits, Indian gooseberry (*Phyllanthus emblica*) fruits,

149 Japanese apricot (*Prunus mume*) fruits, Japanese butterbur (*Petasites japonicus*) stalks,
150 Japanese ginger (*Zingiber mioga*) shoots, Jun-sai (*Bransenia shreberi*) leaves, Kaki persimmon
151 (*Diospyros kaki*) fruits, kiwifruit (*Actinidia deliciosa*) fruits, Korean lettuce (*Lactuca sativa*)
152 leaves, loquat (*Rhaphiolepis bibas*) fruits, lotus (*Nelumbo nucifera*) rhizomes, Mandarin
153 orange (*Citrus unshiu*) fruits, mulkhiya (*Corchorus olitorius*) leaves, okra (*Abelmoschus*
154 *esculentus*) fruits, onion (*Allium cepa*) bulbs, parsley (*Petroselinum crispum*) leaves, pea
155 (*Pisum sativum*) seeds, perilla (*Perilla frutescens* var. *crispa*) leaves, pitaya (*Hylocereus*
156 *undatus*) fruits, plum (*Prunus salicina*) fruits, spinach (*Spinacia oleacea*) leaves, star fruit
157 (*Averrhoa carambola*) fruits, strawberry (*Fragaria* × *ananassa*) achenes, taro (*Colocasia*
158 *esculentai*) tubers, watermelon (*Citrullus lanatus*) fruits, and white radish (*Raphanus*
159 *sativus* var. *hortensis*) roots.

160 ***Plant Extract Preparation*** An edible portion (10 g) taken from a fresh sample was
161 homogenized in 80% (v/v) ethanol (20 mL) using a kitchen blender and filtered through a layer
162 of Miracloth (Sigma-Aldrich Japan). The filtrate was acidified with HCl (10 mM final) to
163 facilitate protein precipitation. It was centrifuged after 10 minutes of incubation at 25˚C, and
164 the resulting supernatant was neutralized with sodium bicarbonate. The volume of
165 deproteinized extract was measured.

166 ***Determination of the Acr-scavenging ability*** A reaction mixture containing 200 μM Acr, 50
167 mM potassium phosphate pH 6.8, and a plant extract was incubated at 30˚C for 10 min. One

168 volume of the mixture was then added to 6.35 volumes of acetonitrile containing 4 mM DNPH
169 and 0.4 M formic acid and incubated at 30˚C for 60 min. The resulting hydrazone solution was
170 filtered through a 0.45 μm filter (Millex LH; Merck, Darmstadt, Germany) and analyzed by
171 HPLC, as follows. The hydrazone solution (10 μL) was injected into a Zorbax ODS column
172 (4.6 × 250 mm, 5 μm; Agilent Technologies Japan, Hachioji, Japan) kept at 40˚C and separated
173 in a 1.0 mL $min^{-1}$ flow of 75% (v/v) acetonitrile in water (isocratic elution) with a high-pressure
174 pump (2690 Separation Module, Waters Corp., Milford, MA). The hydrazone was detected
175 with a UV-visible detector (2487 Absorbance Detector, Waters) at 370 nm. This concentration
176 was chosen based on reported values in Arabidopsis seedlings under salt stress (Sultana et al.
177 2022), corresponding to ~200 μM tissue concentrations, thereby approximating
178 physiologically relevant stress levels.
179 The decrease rate ($v$) of Acr concentration in the reaction mixture (in mol Acr consumed $s^{-1}$ $L^{-}$
180 $^{1}$) was used to calculate the Acr-scavenging ability of the plant extract per unit volume (in mol
181 Acr $s^{-1}$ (L extract)$^{-1}$) by multiplying $v$ by the volume ratio $P$ (reaction mixture/plant extract) as
182 follows:
183 Acr-scavenging ability per unit volume of plant extract (mol $s^{-1}$ (L extract)$^{-1}$)
184 $= v$ (mol Acr scavenged $L^{-1}$ $s^{-1}$) $\times P$

185 The Acr-scavenging ability content in the original sample, as mol Acr consumed $s^{-1}$ (g
186 sample)$^{-1}$, was then calculated from the extraction efficiency $E$ (L extract (g sample)$^{-1}$) as
187 follows:

188 Acr-scavenging ability content (mol $s^{-1}$ (g sample)$^{-1}$)

189 = Acr-scavenging ability of the extract (mol $s^{-1}$ $L^{-1}$) × 1 (L) × $E$ (L extract (g sample)$^{-1}$)

190 ***Purification of the Acr-scavenging component from garlic cloves*** Garlic cloves (40 g) were
191 homogenized in 80% (v/v) ethanol (80 mL) using a kitchen blender, filtered through two layers
192 of Miracloth, and centrifuged to remove insoluble debris. The supernatant was freeze-dried to
193 obtain 7.6 g of material, which was dissolved in distilled water (15 mL) and loaded onto a
194 preparative hydrophilic column (Universal Column Premium Amino 30 μm, 3.0 × 16.5 cm;
195 Yamazen Corp., Osaka, Japan) with a medium pressure chromatography system (EPCLC AI-
196 580; Yamazen Corp.) equipped with a detector (fixed wavelength at 254 nm). Chromatography
197 was performed at a flow rate of 20 mL/min under the following solvent conditions: solvent A:
198 acetonitrile:10 mM ammonium acetate in water (88:12, v/v); solvent B: acetonitrile:100 mM
199 ammonium acetate in water (1:1, v/v). The gradient program consisted of 0–16 min isocratic
200 elution of 0% B, 16–56 min of a linear gradient from 0% to 100% B, and 56–80 min isocratic
201 elution of 100% B. The fraction size was 20 mL. Each fraction was freeze-dried and then
202 dissolved in 2 mL of distilled water, and its Acr-scavenging ability was determined as
203 described above. The most active fraction was then separated on a Unison UK-Amino Column

204 (3 μm, 4.6×100 mm; Imtakt, Kyoto, Japan) with an HPLC apparatus equipped with an LH-40
205 liquid handler and an SPD-10AVP UV-VIS detector (Shimadzu Corp., Kyoto, Japan).
206 Chromatography was performed at a flow rate of 0.6 mL $min^{-1}$ with the following multistep
207 gradient elution: 0–10 min isocratic elution of 0% B; 10–35 min of a linear gradient from 0%
208 to 100% B; 35–50 min isocratic elution of 100% B; 50–55 min of a linear gradient from 100%
209 to 0% B; and, finally, 55–90 min isocratic elution of 0% B. The fraction size was 1.8 mL. The
210 elution profile was monitored at 220 nm for nonspecific detection of organic substances. After
211 40 separation runs (50 μL injection per run), identical fractions were accumulated, freeze-dried,
212 and dissolved in a smaller volume to determine the Acr-scavenging ability.
213 ***LC-MS/MS analysis*** Chromatographic separation was performed on a hydrophilic Intrada
214 Amino Acid column (3 μm, 3 × 100 mm; Imtakt) with a Vanquish UHPLC System (Thermo
215 Fisher Scientific, Waltham, MA). A 5-μL aliquot of the sample was injected into the column
216 and eluted at a flow rate of 0.4 mL $min^{-1}$ under the following solvent conditions: solvent A:
217 0.3% (v/v) in acetonitrile; solvent B: 0.1 M ammonium formate in water:acetonitrile (80:20,
218 v/v). The gradient program was as follows: 0–10 min isocratic elution of 15% B; 10–25 min
219 of a linear gradient from 15% to 60% B; 25–40 min isocratic elution of 60% B; 40–45 min of
220 a linear gradient from 60% to 15% B; and finally 45–50 min isocratic elution of 15% B. The
221 column temperature was set to 40˚C. Mass spectra were acquired using an Orbitrap Exploris
222 120 mass spectrometer (Thermo Fisher Scientific) equipped with an H-ESI source, with

223 acquisition in positive ion mode. The source parameters were as follows: capillary voltage of
224 3.5 kV in positive ion mode, ion transfer tube temperature of 325˚C, vaporizer temperature of
225 350˚C, sheath gas flow of 50 units, auxiliary gas flow of 10 units, and sweep gas of 1 unit. A
226 full scan was performed in the mass-to-charge ratio (*m*/*z*) range of 100–1000, with a resolution
227 of 120,000 at *m*/*z* 200. Tandem MS information was acquired in $tMS^2$ mode with a resolution
228 of 12,000 and HCD collision energies of 15, 30, and 45.
229

230 **Results and Discussion**

231 ***Comparison of Acr-scavenging ability of plants***

232 For choosing a starting material suitable for purifying RCS-scavenging compounds, we first
233 collected various plant samples across diverse angiosperm lineages. To obtain samples in such
234 a variety in short time, we obtained them (46 species in total), mainly fruits and vegetables,
235 from local retail stores (see Materials and Methods). We extracted plants with 80% ethanol
236 because we targeted polar compounds rather than polyphenols, which have been extensively
237 investigated (Colzani, et al., 2018; Huang, et al., 2020; Sugimoto, et al., 2021; Tao, et al.,
238 2019; Wang, et al., 2015; Zhang, et al., 2020; Zhu, et al., 2009). This extract was deproteinized
239 by acid treatment, then neutralized, and its Acr-scavenging rate was determined. To survey
240 RCS scavengers that can react rapidly with Acr, we determined Acr consumption in the initial
241 10 minutes in our assay. The initial Acr concentration was set at 200 μM, mimicking

242 physiological concentration, which was estimated on the following observation. A typical Acr
243 content in salt-stressed *A. thaliana* seedlings is 200 nmol (g fresh weight)$^{-1}$ (Sultana, et al.,
244 2022). From this value, Acr concentration of 200 μM in the tissue was calculated on a simple
245 assumption that the Acr molecules occur in the tissue in a homogenous solution of 1 mL
246 volume per gram tissue weight. The reaction temperature was set at 30˚C to simulate field
247 conditions.

248 Fig. 1 summarizes the Acr-scavenging ability on the fresh weight base of the plant materials.
249 Most plant materials showed significant levels of Acr-scavenging ability, thus indicating that
250 many plants contain Acr-scavenging compounds. The highest Acr-scavenging ability content
251 (in nmol Acr scavenged s$^{-1}$ (g fresh weight)$^{-1}$) were 1.39 for garlic cloves, 0.99 for spinach
252 leaves, 0.96 for avocado fruits, 0.92 for lotus rhizomes, 0.91 for broccoli buds, 0.82 for
253 chestnuts, 0.70 for bamboo shoots, 0.67 for onion bulbs, and 0.65 for both Chinese yam roots
254 and white radish roots. These plants, when placed in the angiosperm phylogeny tree (Cole, et
255 al., 2019), were distributed to different orders of taxa (Fig. 1). We chose garlic cloves as the
256 starting material for purification to identify an Acr-scavenging compound.

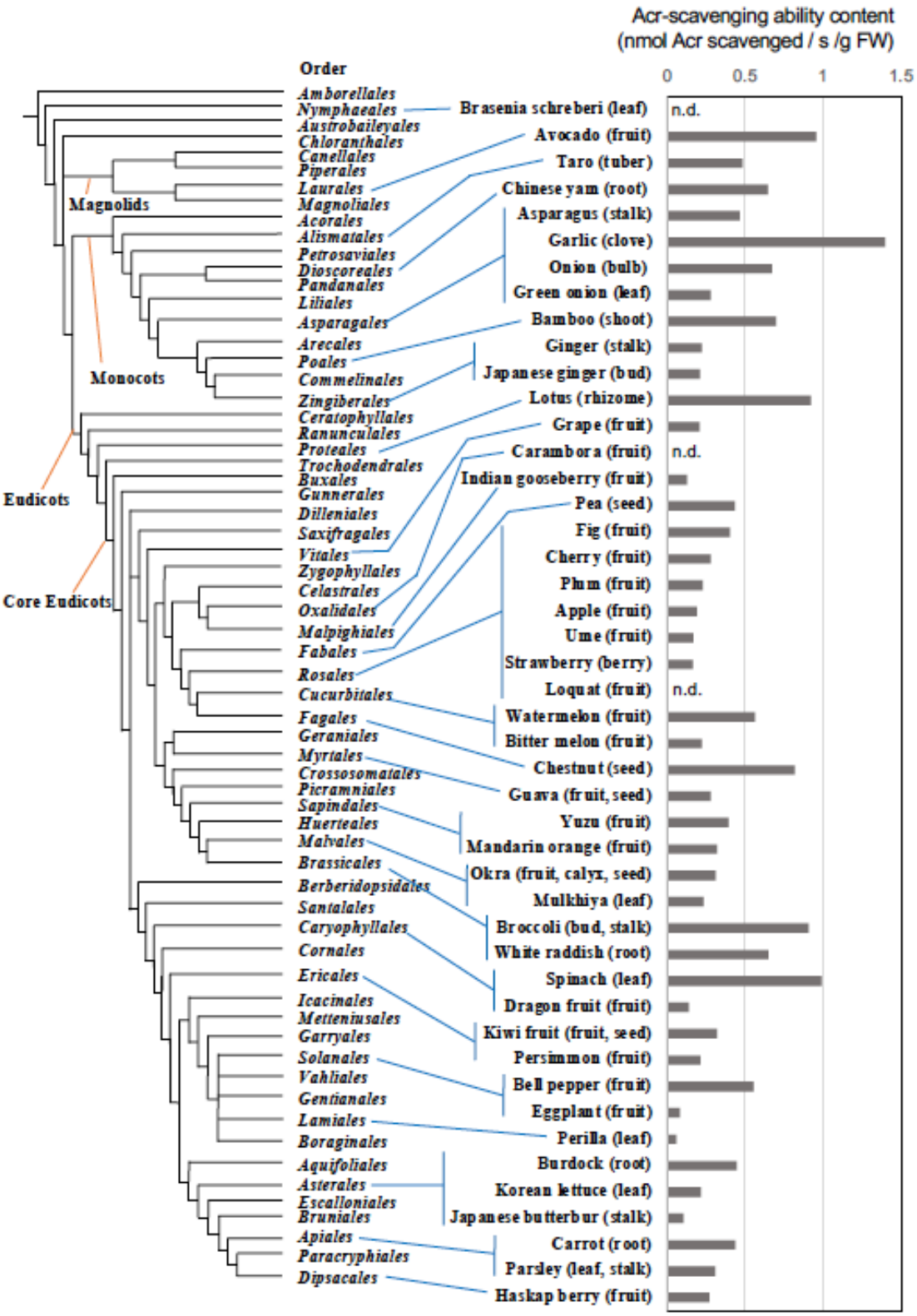


**Figure 1.** Acr-scavenging ability contents of plant materials. Plant extracts (80% ethanol) were deproteinized, neutralized, and tested for the Acr-scavenging ability as in Materials and Methods. Average of two runs. The phylogenic tree was constructed using the Angiosperm Phylogeny Poster (Cole et al. 2019) as a guide.

257

258

259 ***Purification of Acr-scavenging components from garlic extract***

260 Garlic clove extract was first separated by preparative amino column chromatography
261 (Supplementary Fig. S1A), which showed a single prominent peak of Acr-scavenging ability
262 in fractions #13, #14, and #15. We scaled up the sample amount and the column size, as
263 described in the Materials and Methods section, collected the active fractions, concentrated and
264 purified them using an analytical HPLC column. The resulting fraction #8 had a high Acr-
265 scavenging ability (Supplemental Fig. S1B). We then analyzed this fraction by LC-MS/MS.
266 Total ion chromatography (*m*/*z* 100–1000) revealed two major components: a broad peak
267 eluted at 15.3–16.6 min with *m*/*z* 178.0528 and a narrow peak at 18.87 min with *m*/*z* 258.1096
268 (Fig. 2A, black trace).

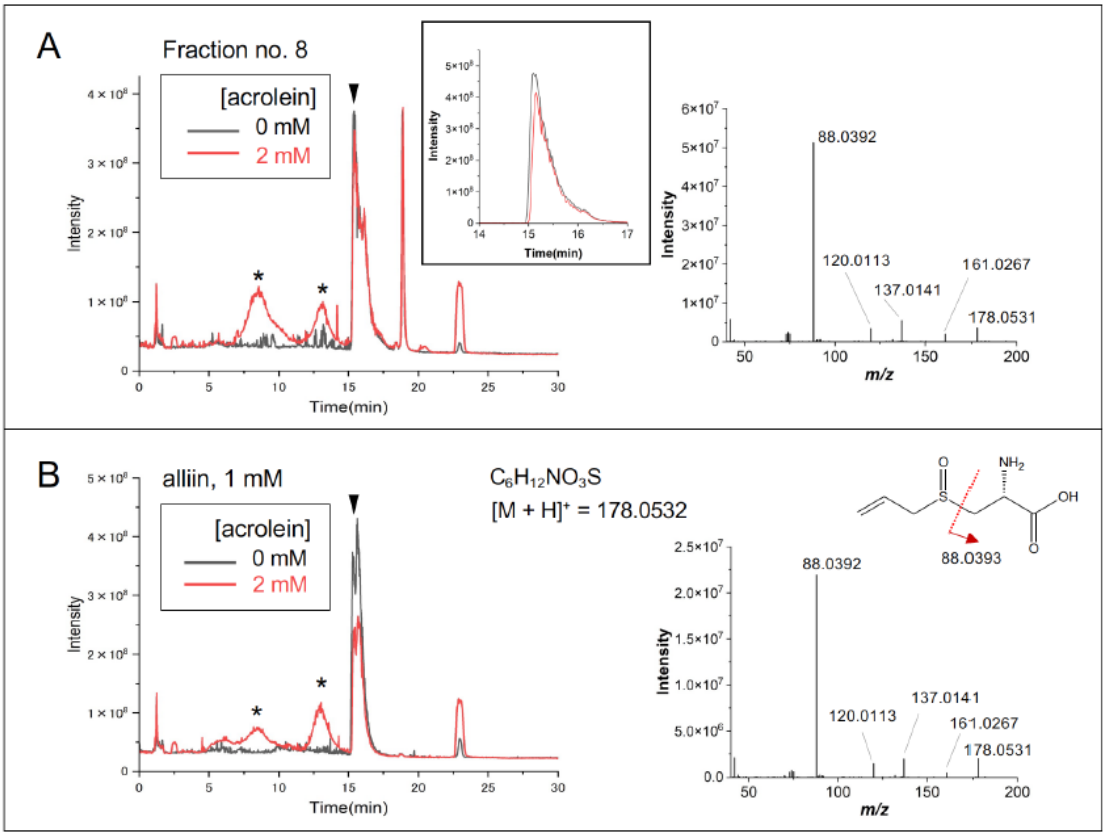


**Figure 2.** LC-MS/MS evidence that alliin is the acrolein-scavenging substance in the fraction no. 8 from the Unizon UK-Amino Column.

To clarify which component is the Acr scavenger, we mixed fraction #8 with Acr and examined the changes in the total ion chromatogram. The addition of Acr at 2 mM resulted in a significant decrease in the 15.3–16.6 min peak (Fig. 2A, inset), while that of the 18.87 min peak was unchanged, thus suggesting that the *m/z* 178.0528 signal represented the Acr scavenger in fraction #8. Addition of Acr to fraction #8 generated two new broad peaks at 8.57 (*m/z* 290.1056) and 13.16 min (*m/z* 234.0795) (Fig. 2A, asterisks). The *m/z* values of these peaks matched hypothetical Acr adducts to the *m/z* 178.0528 compound; the 13.16 min peak

276 corresponded to a mono-Acr adduct (mass increment 56.0265, matching the molecular weight

277 of Acr ($C_3H_4O$)), and the 8.57 min peak a di-Acr adduct (mass increment 112.0526).

278 Assuming that the *m*/*z* 178.0528 ion represents a $[M + H]^+$ ion, the elemental composition

279 of the molecule was deduced as $C_6H_{11}NO_3S$. Retrieval of the corresponding compounds in

280 the databases AraCyc (Mueller, et al., 2003), PlantCyc (Plant Metabolic Network (PMN):

281 https://pmn.plantcyc.org/organism-summary?object=PLANT, on www.plantcyc.org, Jan 15,

282 2022), and KEGG (Kanehisa, et al., 2000) using the software package Compound Discoverer

283 3.0 (Thermo Fisher Scientific), resulted in *S*-allyl-cysteine sulfoxide (alliin; $C_6H_{11}NO_3S$,

284 177.22 g $mol^{-1}$) as the most probable candidate.

285 Alliin is an amino acid sulfoxide characteristic of garlic, accounting for about 30% (w/w) of

286 total free amino acids in garlic cloves (Ueda, et al., 1991), and is a precursor of allicin, the

287 major compound of garlic odor (Stoll and Seebeck, 1948). In the LC-MS/MS analysis,

288 authentic L-alliin eluted as a broad peak ranging from 15.2–16.7 min with an *m*/*z* of 178.0532

289 (Fig. 2B). The $MS^2$ spectrum of this parent ion (*m*/*z* 178.0532) matched the spectrum of the

290 *m*/*z* 178.0528 ion of the Acr scavenger in fraction #8 (Fig. 2A). The addition of Acr to alliin

291 decreased the alliin peak and generated two broad peaks at 8.20 (*m*/*z* 290.1056) and 13.02 min

292 (*m*/*z* 234.0795) (Fig. 2B), as observed for fraction #8. Thus, the Acr-scavenging component in

293 the purified fraction was identified as alliin.

***Reaction mechanism of alliin with Acr*** Uemura et al. (2023) has reported that alliin has a high capacity to scavenge Acr. Its reaction mechanism with Acr, yet to be elucidated, could be similar to that of an amino compound; i.e. the Michael addition of the $\beta$-carbon to the amino nitrogen, and the second addition of Acr to the same nitrogen, followed by the intramolecular aldol condensation to form a nitrogen-containing heterocycle (Carini et al. 2003). When alliin was incubated with Acr, larger MS signals of the mono-Acr adduct (*m/z* 234.0795, eluted at 8.20 min) and the di-Acr adduct (*m/z* 290.1056, 13.02 min) were observed as increasing concentration of Acr (Fig. 3A, B). In addition, another signal at *m/z* 272.0950 arose in higher Acr concentration (Fig. 3C). On the assumption that it represented a $[M + H]^+$ ion, the atomic composition of the compound was deduced as $C_{12}H_{17}NO_4S$. We presumed that this signal corresponded to a dehydrated product of the di-Acr adduct.

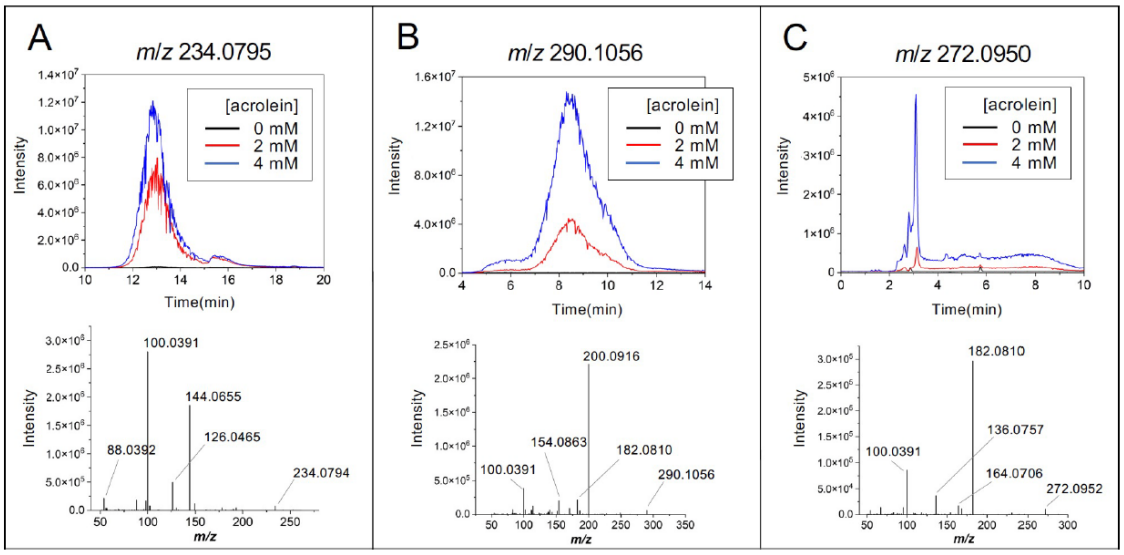


**Figure 3.** LC-MS/MS results of alliin-acrolein adducts.

306 We have purified this putative dehydrated product of the di-Acr adduct and determined its

307 structure with NMR. The deduced structure corresponded to the $N^b$-(3-formyl-3,4-

308 dehydropiperidino) derivative of alliin (Table 1), indicating that the amino group of alliin

309 accepted two molecules of Acr, as expected. Specifically, one Acr molecule adds to the amino

310 group (Michael-type reaction), then the resulting secondary amino group undergoes Michael

311 addition with another Acr molecule to form the $(Acr)_2$ adduct, which then undergoes aldol

312 condensation to form a nitrogen-containing heterocycle (Figure 4). The $MS^2$ spectra for the

313 Acr adducts support this mechanism; the spectrum for the mono-Acr adduct contained a

314 product ion at *m/z* 144.0655, the deduced atomic composition for which ($C_6H_{10}NO_3$) matched

315 the fragment generated by cleavage between the sulfur atom and the *β*-carbon of the amino

316 acid, the same cleavage position as in alliin (Fig. 2B). Similarly, the $MS^2$ spectra of the di-Acr

**Table 1.** $^1$H NMR (400 MHz) and $^{13}$C NMR (500 MHz) chemical shift data of the purified adduct of *m/z* 272.0950. Deduced structure of the dehydrated product of $(Acr)_2$-alliin adduct and a possible LC-MS/MS fragment ion structure are shown.

| NMR data | | | Structural formula of the dehydrated product of $(Acr)_2$-alliin adduct | Fragment ion (+) of LC-MS/MS |
|---|---|---|---|---|
| No. | $\delta_H$ | $\delta_C$ | | |
| 1 | 5.52 | 124.85 | | |
| 2 | 5.94 | 125.03 | | |
| 3 | 3.60, 3.80 | 54.2 | | |
| 4 | 3.27, 3.33 | 49.97 | | |
| 5 | 3.7 | 63.68 | | |
| 6 | - | 174.82 | | |
| 7 | 2.87, 3.06 | 45.9 | | |
| 8 | 2.61 | 26.81 | | |
| 9 | 7.18 | 152.41 | **exact mass 271.08728** | ***m/z* 182.0810** |
| 10 | - | 138.06 | | |
| 11 | 9.35 | 195.6 | | |
| 12 | 3.5 | 45.48 | | |

317 adduct and its dehydrated product contained product ions at *m/z* 200.0917 (Fig. 3B) and *m/z*

318 182.0811 (Fig. 3C), which correspond to the fragments at the same cleavage position of the

319 deduced compounds, respectively. This formation parallels mechanisms described for

320 histidine-containing dipeptides (Carini et al. 2003), where successive Michael additions are

321 followed by intramolecular condensation (Figure 4).

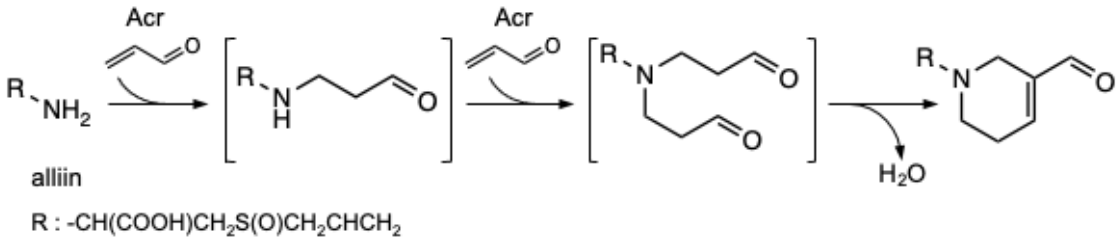


**Figure 4.** Possible reactions of alliin (R-$NH_2$) with Acr.

322

323

324 ***Comparison of the Acr-scavenging ability of S-alk(en)yl cysteine sulfoxides, amino***

325 ***compounds, and polyphenols*** Plants in the *Allium* family are rich in alliin-analogous *S*-

326 alk(en)yl cysteine sulfoxides, such as *S*-propenylcysteine sulfoxide (isoalliin) in onion (*A.*

327 *cepa*) and *S*-methylcysteine sulfoxide (methiin) in Oriental garlic (*A. tuberosum*) (Yamazaki,

328 et al., 2011). Isoalliin and methiin also formed mono-Acr and $(Acr)_2$ adducts and the

329 dehydration product of the $(Acr)_2$ adduct, as did alliin (Supplementary Fig. S3 and S4). The

330 Acr-scavenging rates of these *S*-alk(en)yl cysteine sulfoxides were 120–150 μM Acr in 30 min,

331 when the reaction was started with 1 mM Acr and 1 mM scavenger (Table 2A). These rates

332 were comparable to, or even higher than, those for carnosine and anserine, Acr-scavenging
333 dipeptides in animals (Carini, et al., 2003; Spaas, et al., 2021).
334 As compared with broader variety of amino compounds, these *S*-alk(en)yl cysteine sulfoxides
335 excelled GABA and most of protein-constituting amino acids such as Met, His, Lys, Arg and
336 Gly for the Acr-scavenging rate. Such high Acr-scavenging rate for *S*-alk(en)yl cysteine
337 sulfoxides appears to be attributed to the presence of sulfoxide close to the amino carbon.
338 Indeed, methionine sulfoxide, in which the sulfoxide is one carbon further away, showed a
339 significantly faster Acr-scavenging rate than other amino acids lacking a sulfoxide although its
340 rate was slower than *S*-alk(en)yl cysteine sulfoxides (Table 2A).
341 We also compared the *S*-alk(en)yl cysteine sulfoxides with polyphenols that can scavenge
342 Acr. Isoalliin, methiin and alliin outperformed EGCG in scavenging Acr (Table 2A). We note
343 that assays of polyphenols (resveratrol, hesperetin) were conducted in 10% DMSO with longer
344 incubation times due to low solubility and slower reaction kinetics (Wang, et al., 2015).
345 Therefore, direct quantitative comparisons with amino acid sulfoxides should be made
346 cautiously. To compare alliin with resveratrol and hesperetin, a separate experiment was
347 performed in 10% DMSO solution and reaction time was set to 5 h (Table 2B). Under these
348 conditions, alliin scavenged Acr faster than EGCG, resveratrol, and hesperetin. Theophylline,
349 another type of Acr scavenger (Jiang, et al., 2020b) showed an Acr-scavenging rate comparable
350 to that for hesperetin and much slower than that for EGCG and alliin (Table 2B).

351

352 **Table 2** (A) Comparison of Acr-scavenging rate of amino compounds. Acr (1 mM) was
353 incubated with a scavenger (1 mM) in 50 mM potassium phosphate, pH 7.0, at 30˚C for 30
354 min. The remaining Acr was determined by HPLC after derivatization with DNPH, as
355 described in the Materials and Methods section. Acr consumption (concentration in the
356 reaction mixture) in 30 min is shown. (B) Comparison of Acr-scavenging rate for alliin,
357 polyphenols, and theophylline. Acr (1 mM) was incubated with a scavenger (1 mM) in 10%
358 DMSO, 50 mM potassium phosphate, pH 7.0, at 30˚C for 5 h. Acr consumption in 5 h is
359 shown. The values shown are the average and standard error of three independent runs.
360 Different letters in the Statistics column represent significantly different values ($P < 0.05$,
361 Tukey's test).

| **A** | Compound | Acr consumption (μM in 30 min) | Statistics |
|---|---|---|---|
| | Isoalliin | 153.8 ± 6.5 | a |
| | Methiin | 144.5 ± 14.0 | ab |
| | Alliin | 126.8 ± 5.4 | bc |
| | Carnosine | 114.3 ± 1.3 | cd |
| | Anserine | 99.4 ± 5.5 | de |
| | Methionine sulfoxide | 86.0 ± 8.3 | e |
| | Histidine | 63.9 ± 6.0 | f |
| | Lysine | 59.5 ± 8.9 | f |
| | Phenylalanine | 57.5 ± 0.9 | f |
| | EGCG | 45.4 ± 5.2 | f |
| | Arginine | 44.7 ± 6.3 | f |
| | Histamine | 40.1 ± 8.4 | fg |
| | Methionine | 22.7 ± 8.7 | gh |
| | GABA | 10.6 ± 5.9 | h |
| | *β*-Alanine | 6.5 ± 3.7 | h |

362

| **B** | Compound | Acr consumption (μM in 5 h) | Statistics |
|---|---|---|---|
| | Alliin | 419.1 ± 3.0 | a |
| | EGCG | 282.0 ± 4.6 | b |
| | Resveratrol | 31.8 ± 1.5 | c |
| | Hesperetin | 18.9 ± 1.0 | d |
| | Theophylline | 17.9 ± 3.6 | d |

363

364 ***RCS scavenging compounds are present in many plant species*** Because RCS are secondary
365 toxic products derived from ROS, plants have evolved multiple enzymatic and non-enzymatic
366 mechanisms to mitigate their harmful effects (Mano et al. 2019a,b). In this study, we
367 established a method to evaluate the RCS-scavenging ability of plant extracts and demonstrated
368 that *S*-alk(en)yl cysteine sulfoxides, amino acids characteristic of *Allium* family, are highly
369 efficient Acr scavengers. Among them, isoalliin, the major sulfoxide in onion, exhibited the
370 strongest Acr-scavenging activity, surpassing not only its structural analog alliin but also other
371 well-known plant-derived and animal-derived scavengers. This finding identifies isoalliin as a
372 representative plant RCS scavenger and underscores the contribution of *Allium* metabolites to
373 the chemical defense system against carbonyl stress. Isoalliin concentrations in onion bulbs are
374 reported at 5–20 μmol $g^{-1}$ FW (Yamazaki et al. 2011; Ueda et al. 1991). At these levels,
375 isoalliin would be comparable to stress-induced Acr accumulation, supporting its role as an in
376 planta scavenger.

377 It is noteworthy that the presence of a sulfoxide group in close proximity to the amino
378 carbon markedly enhances the Michael acceptor reactivity of the amino group, thereby
379 conferring the high RCS-scavenging capacity observed in S-alk(en)yl cysteine sulfoxides.
380 Consequently, the RCS-scavenging property of a compound appears to be governed by the
381 cooperative action of two or more functional groups, rather than by the reactivity of a single

382 moiety alone. More broadly, our findings suggest that structurally diverse, and as yet
383 unexplored, plant metabolites may play critical roles in mitigating oxidative damage through
384 RCS detoxification.
385
386
387 **ABBREVIATIONS**
388 Acr, acrolein; DNP-, dinitrophenylhydrazo-; DNPH, 2,4-dinitrophenylhydrazine; FW, fresh
389 weight; GSH, the reduced form of glutathione; HNE, 4-hydroxy-(*E*)-2-nonenal; LOOH, lipid
390 peroxide; RCS, reactive carbonyl species; ROS, reactive oxygen species.
391
392 **AUTHOR CONTRIBUTION**
393 Conceptualization: J. M. and D.S.; Investigation: A.H., N.T.; Methodology: J.M., C.N., A.H.,
394 N.T., Y.M., K.M.; Roles/Writing - original draft: A.H., N.T., Writing - review & editing; A.H.,
395 J.M., Funding acquisition: J.M., D.S.; Supervision: J.M.
396
397 **ACKNOWLEDGMENT**
398 The authors would like to express their gratitude to Ryoma Oishi and Suzuka Monden for their
399 technical assistance and to Prof. Toshihiro Murafuji, Yamaguchi University, for discussion.
400

401 **FUNDING**

402 This work was supported by the Ministry of Agriculture, Forestry and Fisheries of Japan, by

403 KAKENHI Grants (nos. 17K19909 and 20H03278) from the Japan Society for the Promotion

404 of Science (to J. M.), and by Yamaguchi University Project for Formation of the Core Research

405 Project. This work resulted from the use of research equipment shared in the MEXT Project

406 for promoting public utilization of advanced research infrastructure (Program for supporting

407 the construction of core facilities) Grant Number JPMXS0440400022.

408

409 **FIGURE CAPTIONS**

410 **Fig 1.** Acr-scavenging ability contents of plant materials. Plant extracts (80% ethanol) were

411 deproteinized, neutralized, and tested for the Acr-scavenging ability as in Materials and

412 Methods. Average of two runs. The phylogenic tree was constructed using the Angiosperm

413 Phylogeny Poster (Cole et al. 2019) as a guide.

414 **Fig. 2.** LC-MS/MS evidence that alliin is the Acr-scavenging substance in fraction #8 using a

415 Unizon UK-Amino Column. A: Total ion chromatograms (*m*/*z* range 100–1000) of fraction

416 #8 with 2 mM Acr (red trace) and without it (black). The MS/MS spectrum of the *m*/*z*

417 178.0528 signal at 15.4 min is shown on the right. Inset: expanded chromatogram of the 15.1

418 min peak. B: Total ion chromatograms (*m*/*z* range 100–1000) of 1 mM alliin with 2 mM Acr

419 (red trace) and without it (black). The MS/MS spectrum of the *m*/*z* 178.0532 signal at 15.4

420 min (arrowhead) is shown on the right. Asterisks show possible Acr reaction products with

421 the scavenging compound (A) or with alliin (B).

422 **Fig. 3.** LC-MS/MS results for alliin-Acr adducts. An authentic alliin preparation (5 mM) was

423 mixed with various concentrations of Acr, incubated for 1 h, and subjected to LC-MS/MS

424 analysis. A: Extracted ion chromatograms of the mono-Acr adduct of alliin (*m*/*z* 234.0795). B:

425 Extracted ion chromatograms of the $(Acr)_2$ adduct (*m*/*z* 290.1056). C: Extracted ion

426 chromatograms of the dehydrated products from the di-Acr adduct (*m*/*z* 272.0950). The

427 corresponding parent ion MS/MS spectrum is shown at the bottom of panels A–C. This

428 formation parallels mechanisms described for histidine-containing dipeptides (Carini et al.

429 2003), where successive Michael additions are followed by intramolecular condensation.

430 Figure 4 illustrates this comparison explicitly.

431 **Fig. 4.** Possible reactions of alliin with Acr.

432

433 **ASSOCIATED CONTENTS**

434 Supporting information is available.

435 Two chromatographic results for the purification of Acr-scavenging substances from garlic

436 extract (Fig. S1), MS spectrum of the 15.42 min peak of fraction #8 (Fig. S2), LC-MS/MS

437 results for the reaction products of isoalliin and Acr (Fig. S3), and LC-MS/MS results for the

438 reaction products of methiin and Acr (Fig. S4).

441 **REFERENCES**

442 Aldini, G., Carini, M., Beretta, G., Bradamante, S., and Facino, R. M. (2002) Carnosine is a
443 quencher of 4-hydroxy-nonenal: through what mechanism of reaction? Biochem.
444 Biophys. Res. Commun. 298: 699-706.

445 Aldini, G., Facino, I., Beretta, G. and Carini, M. (2005) Carnosine and related dipeptides as
446 quenchers of reactive carbonyl speices: From structural studies to therapeutic
447 perspecitves. BioFactors 24: 77-87.

448 Aldini, G., Dalle-Donne, I., Facino, R. M., Milzani, A. and Carini, M. (2007) Intervention
449 strategies to inhibit protein carbonylation by lipoxidation-derived reactive carbonyls.
450 Med. Res. Rev. 27: 817-868, https://doi.org/10.1002/med.20073.

451 Aldini, G., Orioli, M., Rossoni, R., Savi, F., Braidotti, P., Vistoli, G., Yeum, K.-J., Negrisoli,
452 G. and Carini, M. (2011) The carbonyl scavenger carnosine ameliorates dyslipidaemia
453 and renal function in Zucker obese rats. J. Cell. Mol. Med. 15: 1339-1354.

454 Asada, K. (2006) Production and scavenging of reactive oxygen species in chloroplasts and
455 their functions. Plant Physiol. 141: 391-396.

456 Biswas, M. S. and Mano, J. (2015) Lipid peroxide-derived short-chain carbonyls mediate
457 hydrogen peroxide-induced and salt-induced programmed cell death in plants. Plant
458 Physiol. 168: 885–898.

459 Carini, M., Aldini, G., Beretta, G., Arlandini, E. and Facino, R. M. (2003) Acrolein-
460 sequestering ability of endogenous dipeptides: characterization of carnosine and
461 homocarnosine/acrolein adducts by electrospray ionization tandem mass
462 spectrometry. J. Mass Spectr. 38: 996-1006.

463 Cole, T. C., Hilger, H. H. and Stevens, P. (2019) Angiosperm Phylogeny Poster (APP) –
464 Flowering plant systematics. PeerJ Preprints 7: e2320v6

465 Colzani, M., Regazzoni, L., Criscuolo, A., Baron, G., Carini, M., Vistoli, G., Lee, Y.-M., Han,
466 S. I., Aldini, G. and Yeum, K.-J. (2018) Isotopic labelling for the characterisation of
467 HNE-sequestering agents in plant-based extracts and its application for the
468 identification of anthocyanidins in black rice with giant embryo. Free Rad. Res. 52:
469 896-906.

470 Esterbauer, H., Zollner, H. and Scholtz, N. (1975) Reaction of glutathione with conjugated
471 carbonyls. Z. Naturforsch. 30c 466-473.

472 Esterbauer, H., Schaur, R. and Zollner, J. H. (1991) Chemistry and biochemistry of 4-
473 hydroxynonenal, malonaldehyde and related aldehydes. Free Rad. Biol. Med. 11: 81-
474 128.

475 Foyer, C. H. and Noctor, G. (2003) Redox sensing and signalling associated with reactive
476 oxygen in chloroplasts, peroxisomes and mitochondria. Physiol. Plant. 119 355-364.

477 Huang, Q., Zhu, Y., Lv, L. and Sang, S. (2020) Translating in vitro acrolein-trapping capacities
478 of tea polyphenol and soy genistein to in vivo situations is mediated by the
479 bioavailability and biotransformation of individual polyphenols. Mol. Nutr. Food Res.
480 64: 1900274.

481 Jiang, K., Yin, Z., Zhou, P., Guo, H., Huang, C., Zhang, G., Hu, W., Ou, S. and Ou, J. (2020a)
482 The scavenging capacity of γ-aminobutyric acid for acrolein and the cytooxicity of the
483 formed adduct. Food Funct. 11: 7736.

484 Jiang, X., Zhang, D., Lu, Y. and Lv, L. (2020b) Acrolein-trapping mechanism of theophylline
485 in green tea, coffee, and cocoa: Speedy and successful. J. Agric. Food Chem. 68: 9718-
486 9724.

487 Kanehisa, M. and Goto, S. (2000) KEGG: Kyoto Encyclopedia of Genes and Genomes.
488 Nucleic Acids Res. 28: 27-30.

489 Knieper, M., Viehhauser, A. and Dietz, K.-J. (2023) Oxylipins and reactive carbonyls as
490 regulators of the plant redox and reactive oxygen species network under stress.
491 Antioxidants 12: 814.

492 Liu, Y., Xu, G. and Sayre, L. M. (2003) Carnosine 1nhibits (*E*)-4-hydroxy-2-nonenal-induced
493 protein cross-linking: structural characterization of carnosine−HNE adducts. Chem.
494 Res. Toxicol. 16: 1589-1597.

495 Mano, J. (2012) Reactive carbonyl species: their production from lipid peroxides, action in
496 environmental stress, and the detoxification mechanism. Plant Physiol. Biochem. 59:
497 90-97.

498 Mano, J., Torii, Y., Hayashi, S.-I., Takimoto, K., Matsui, K., Nakamura, K., Inzé, D.,
499 Babiychuk, E., Kushnir, S. and Asada, K. (2002) The NADPH:quinone
500 oxidoreductase P1-ζ-crystallin in Arabidopsis catalyzes the α,β-hydrogenation of 2-
501 alkenals: detoxication of the lipid peroxide-derived reactive aldehydes. Plant Cell
502 Physiol. 43:1445-1455.

503 Mano, J., Belles-Boix, E., Babiychuk, E., Inzé, D., Torii, Y., Hiraoka, E., Takimoto, K.,
504 Slooten, L., Asada, K. and Kushnir, S. (2005) Protection against photooxidative injury
505 of tobacco leaves by 2-alkenal reductase. Detoxication of lipid peroxide-derived
506 reactive carbonyls. Plant Physiol. 139: 1773–1783.

507 Mano, J., Tokushige, K., Mizoguchi, H., Fujii, H. and Khorobrykh, S. (2010) Accumulation
508 of lipid peroxide-derived, toxic α,β-unsaturated aldehydes (E)-2-pentenal, acrolein
509 and (E)-2-hexenal in leaves under photoinhibitory illumination. Plant Biotechnol. 27:
510 193–197.

511 Mano, J., Ishibashi, A., Muneuchi, H., Morita, C., Sakai, H., Biswas, M. S., Koeduka, T. and
512 Kitajima, S. (2017) Acrolein-detoxifying isozymes of glutathione transferase in
513 plants. Planta 245: 255-264.

514 Mano, J., Kanameda, S., Kuramitsu, R., Matsuura, N. and Yamauchi, Y. (2019)
515 Detoxification of reactive carbonyl species by glutathione transferase Tau isozymes.
516 Front. Plant Sci. 10: 487.
517 Mano, J., Biswas, M. S. and Sugimoto, K. (2019) Reactive carbonyl species: A missing link in
518 ROS signaling. Plants 8: 391.

519 Mueller, L. A., Zhang, P. and Rhee, S. Y. (2003) AraCyc: A biochemical pathway database for
520 Arabidopsis. Plant Physiol. 132: 453-460.

521 Nurbekova, Z., Srivastava, S., Standing, D., Kurmanbayeva, A., Bekturova, A., Soltabayeva,
522 A., Oshanova, D., Turečková, V., Strand, M., Biswas, M. S., Mano, J. and Sagi, M.
523 (2021) Arabidopsis aldehyde oxidase 3, known to oxidize abscisic aldehyde to ABA,
524 protects leaves from aldehyde toxicity. Plant J. 108: 1439-1455.
525 Roach, T., Stöggl, W., Baur, T. and Kranner, I. (2018) Distress and eustress of reactive
526 electrophiles and relevance to light stress. Free Rad. Biol. Med., 122: 65-73.

527 Schauenstein, E., Esterbauer, H. and Zollner, H. (1977) Aldehyde in Biological Systems: Their
528 Natural Occurrence and Biological Activities. Pion, pp. 589–590.

529 Song, X., Lu, Y., Lu, Y. and Lv, L. (2021) Adduct formation of acrolein with cyanidin-*O*-
530 glucoside and its degradants/metabolites during thermal processing or in vivo after
531 consumption of red bayberry. J. Agric. Food Chem. 69: 13143-13154.

532 Spaas, J., Franssen, W. M. A., Keytsman, C., Blancquaert, L., Vanmierlo, T., Bogie, J., Broux,
533 B., Hellings, N., van Horssen, J., Posa, D. K., Hoetker, D., Baba, S. P., Derave, W. and
534 Eijnde, B. O. (2021) Carnosine quenches the reactive carbonyl acrolein in the central
535 nervous system and attenuates autoimmune neuroinflammation. J. Neuroinflam., 18:
536 255.

537 Srivastava, S., Brychkova, G., Yarmolinsky, D., Soltabayeva, A., Samani, T. and Sagi, M.
538 (2017) Aldehyde oxidase 4 plays a critical role in delaying silique senescence by
539 catalyzing aldehyde detoxification. Plant Physiol. 173: 1977–1997.

540 Stoll, A. and Seebeck, E. (1948) Über Alliin, die genuine Muttersubstanz des Knoblauchöls. 1.
541 Mitteilung über Allium-Substanzen. Helv. Chim. Acta 31: 189-210.

542 Sugimoto, K., Matsuoka, Y., Sakai, K., Fujiya, N., Fujii, H. and Mano, J. (2021) Catechins in
543 green tea powder (matcha) are heat-stable scavengers of acrolein, a lipid peroxide-
544 derived reactive carbonyl species. Food Chem. 355: 129403.

545 Sultana, M. S., Yamamoto, S.-I., Biswas, M. S., Sakurai, C., Isoai, H. and Mano, J. (2022)
546 Histidine-containing dipeptides mitigate salt stress in plants by scavenging reactive
547 carbonyl species. J. Agric. Food Chem. 70: 11169-11178.

548 Sultana, M. S., Sakurai, C., Biswas, M. S., Szabados, L. and Mano, J. (2024) Accumulation of
549 reactive carbonyl species in roots as the primary cause of salt stress-induced growth
550 retardation of *Arabidopsis thaliana*. Physiol. Plant. 176: e14198.

551 Sunkar, R., Bartels, D. and Kirch, H.-H. (2003) Overexpression of a stress-inducible
552 aldehyde dehydrogenase gene from *Arabidopsis thaliana* in transgenic plants
553 improves stress tolerance. Plant J. 35: 452–464,.

554 Tao, Z.-h., Li, C., Xu, X.-f. and Pan, Y.-j. (2019) Scavenging activity and mechanism study of
555 ferulic acid against reactive carbonyl species acrolein. J. Zhejiang Univ.-Science B 20:
556 868-876.

557 Ueda, Y., Kawajiri, H., Miyamura, N. and Miyajima, R. (1991) Content of some sulfur-
558 containing components and free amino acids in various strains of garlic. Nippon
559 Shokuhin Kogyo Gakkaishi 38: 429-434.

560 Uemura, T., Uchida, M., Nakamura, M., Shimekake, M., Sakamoto, A., Terui, Y., Higashi, K.,
561 Ishii, I., Kashiwagi, K. and Igarashi, K. (2023) A search for acrolein scavengers among
562 food components. Amino Acids 55: 509-518.

563 Wang, W., Qi, Y., Rocca, J. R., Sarnoski, P. J., Jia, A. and Gu, L. (2015) Scavenging of toxic
564 Acrolein by resveratrol and hesperetin and identification of adducts. J. Agric. Food
565 Chem. 63: 9488-9495.

566 Wible, R. S. and Sutter, T. R. (2017) Soft cysteine signaling network: the functional
567 significance of cysteine in protein function and the soft acids/bases thiol chemistry that
568 facilitates cysteine modification. Chem. Res. Toxicol. 30: 729-762.

569 Yamauchi, Y., Hasegawa, A., Taninaka, A., Mizutani, M. and Sugimoto, Y. (2011) NADPH-
570 dependent reductases involved in the detoxification of reactive carbonyls in plants. J.
571 Biol. Chem. 286: 6999–7009.

572 Yamauchi, Y., Hasegawa, A., Mizutani, M. and Sugimoto, Y. (2012) Chloroplastic NADPH-
573 dependent alkenal/one oxidoreductase contributes to the detoxification of reactive
574 carbonyls produced under oxidative stress. FEBS Lett. 586: 1208-1213.

575 Yamazaki, Y., Iwasaki, K., Mikami, M. and Yogihashi, A. (2011) Distribution of eleven
576 flavor precursors, *S*-alk(en)yl-L-cysteine derivatives in seven Allium vegetables. Food
577 Sci. Technol. Res. 17: 55-62.

578 Yin, L., Mano, J., Wang, S., Tsuji, W. and Tanaka, K. (2010) The involvement of lipid
579 peroxide-derived aldehydes in aluminum toxicity of tobacco roots. Plant Physiol. 152:
580 1406–1417.

581 Zhang, D., Jiang, X., Xiao, L., Lu, Y., Sang, S., Lv, L. and Dong, W. (2020) Mechanistic
582 studies of inhibition on acrolein by myricetin. Food Chem. 323: 126788.

583 Zhu, Q., Zheng, Z.-P., Cheng, K.-W., Wu, J.-J., Zhang, S., Tang, Y. S., Sze, K.-H., Chen, J.,
584 Chen, F. and Wang, M. (2009) Natural polyphenols as direct trapping agents of lipid
585 peroxidation-derived acrolein and 4-hydroxy-trans-2-nonenal. Chem. Res. Toxicol. 22:
586 1721-1727.

587 Zou, Z., Yin, Z., Ou, J., Zheng, J., Liu, F., Huang, C. and Ou, S. (2021) Identification of adducts
588 formed between acrolein and alanine or serine in fried potato crips and the cytotoxicity-
589 lowering effect of acrolein in three cell lines. Food Chem. 361: 130164.

590

591 **Declaration of generative AI and AI-assisted technologies in the writing process**

592 During manuscript preparation, the authors used AI-based language tools (DeepL, ChatGPT,
593 Google Gemini) solely for improving English grammar and readability. All scientific content
594 was conceived, verified, and revised by the authors, who take full responsibility for the
595 manuscript.

596

597

598